High Efficient 820 nm MOS Ge Quantum Dot Photodetectors for Short-Reach Integrated Optical Receivers with 1300 and 1550 nm Sensitivity

B.-C. Hsu[a], S. T. Chang[a], C.-R. Shie[a], C.-C. Lai[a], P. S. Chen[b], and C. W. Liu[a,b]

[a] Graduate Institute of Electronics Engineering and Department of Electrical Engineering,
National Taiwan University, Taipei, Taiwan, R. O. C.
[b] ERSO/ITRI, Hsinchu, Taiwan, R. O. C.
E-mail: chee@cc.ee.ntu.edu.tw

Abstract

A metal-oxide-semiconductor (MOS) Ge quantum dot photodetector is demonstrated. The oxide is grown directly on Ge substrate by liquid phase deposition (LPD). The photodetector has the responsivity of 130, 0.16, and 0.08 mA/W under the wavelength of 820 nm, 1300 nm, and 1550 nm, respectively. The dark current is extremely low (0.06 mA/cm^2). The high performance of Ge quantum dot MOS photodetectors at 820 nm makes it feasible to integrate optoelectronic devices into the Si chip for short-reach optical communication.

Introduction

The interest of silicon-based optoelectronic devices grows rapidly in the last decade (1). However, due to the large absorption length (~16 μm) of Si at 820 nm (2) and the forbidden absorption at 1300 and 1550 nm, the Si-based photodetector has limited detection efficiency and wavelength range. The incorporation of Ge into Si can not only increase the cut-off wavelength, but also enhance the absorption efficiency (small absorption length). The strained Ge could have an absorption length of 0.1 μm or less at the wavelength of 820 nm. In this paper, we use the metal-oxide-semiconductor (MOS) tunneling structure (3) with Ge quantum dot to implement the photodetector at 820 nm with high responsivity and extremely low dark current (<1 mA/cm^2). The low temperature (~50 ℃) liquid phase deposited (LPD) SiO_2 is used as gate dielectric material to avoid the high temperature thermal oxidation, which induces the Ge-related defects during oxidation. A 5-layer Ge quantum dots with ~2 nm wetting layers is used as a light absorbing layer, together with Si, Ge, and a $Si_{0.8}Ge_{0.2}$ multi-layer structure for comparison.

Strained SiGe/Ge

Fig. 1 shows the bandgap and cut-off wavelength vs strained and relaxed Ge mole fraction. As Ge mole fraction increases, the maximum absorption wavelength also increases. The shadowed area represents the laser bandwidth in our experiment. Fig. 2 shows the absorption length at 820, 1300, and 1550 nm vs Ge mole fraction. The absorption length decreases as the Ge mole fraction increases. For the large Ge fraction, the shadowed areas indicate the uncertainty of the estimation. The incorporation of strained Ge/SiGe into optoelectronic devices makes devices particularly useful over the important fiber optic communications wavelengths, and can be applied to the fiber optic communications.

Ge Quantum Dots Fabrication

The Si/Ge quantum dots are prepared by UHVCVD (ultra high vacuum chemical vapor deposition) on p-type Si (001) substrates. The structure is shown in Fig. 5(a). After Si buffer layer of 50 nm was grown, 5 periods of Ge/Si bilayers were grown to form the self-assembled Ge dots at temperature of 600 °C under the Stranski-Krastanov (SK) growth mode (4). The Ge layers are separated by 50 nm Si spacer layers. A 3 nm (nominal thickness) Si cap was deposited above the top layer of self-assembled Ge layer as the starting layer for the subsequent LPD oxide deposition. All UHVCVD layers are p-type with the estimated concentration on the order of 1×10^{16} cm^{-3}. For comparison, RTO (Rapid Thermal Oxidation) was also performed. As a result, the LPD oxide yields larger external quantum efficiency than the rapid thermal oxide (Fig. 3).

Liquid Phase Deposition Oxide

To avoid material degradation such as strain relaxation and Ge out diffusion, the low temperature oxide is often required to reduce the thermal budget of SiGe device process. LPD is a promising low-temperature process for SiO_2 formation with the low thermal budget and low cost. A simplified mechanism of LPD growth was originally proposed by Nagayama et al. (5) based on the reaction of H_2SiF_6 with water to form hydrofluoric acid and solid SiO_2.

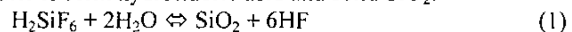

$$H_2SiF_6 + 2H_2O \Leftrightarrow SiO_2 + 6HF \quad (1)$$

However, the time for solution preparation was too long in this LPD process. Therefore, we used the LPD method with short preparation time (6). The experimental flow diagram for the LPD process is illustrated in Fig. 4. First, the silicic acid (SiO_2:$x$$H_2O$) was added to hydrofluosilicic acid (H_2SiF_6, 3 mol/l) at the temperature of 35℃. The solution was then stirred for 3 hrs. Next, the solution was filtered to remove the undissolved silica. H_2O was then added to the saturated

0-7803-7462-2/02/$17.00 ©2002 IEEE

solution. Si, Ge, Ge quantum dot, and $Si_{0.8}Ge_{0.2}$ multi-layer structure were used in this experiment. The native oxide was removed by dipping in diluted HF solution before the LPD process. The substrates were then placed into the immersing solution at 50℃. One interesting observation of LPD oxide on Ge quantum dot samples is that SiO_2 dots are formed directly on Ge dots, as shown in Fig. 5(b) and Fig. 6. The tensile strain field on the Si cap of self-assembled quantum dots can have preferential oxide deposition during LPD process. The oxide dots are formed on the tensile strained area of Si cap, and are aligned vertically with Ge dots embedded in the Si caps.

Photodetector

Fig. 7 shows the typical dark and photo current of a Ge quantum dot detector on p-type substrate. The fiber is pointed to the edge of the gate electrode and the photo-generated carriers can be collected by electrode by lateral drift and diffusion, as shown in the inset of Fig. 7. Note that the photocurrent is relatively independent of applied voltage, and the device can operate close to zero volt bias. Fig. 8 shows the band diagram of a Ge quantum dot NMOS detector under inversion bias. The deep depletion region is formed at inversion bias due to the tunneling of LPD oxide. The photoelectrons are generated in the deep depletion region, and are swept toward the gate electrode. The photoelectrons tunnel from the active layers to the Al gate electrode through the trap-assisted tunneling of LPD oxide. Since the band offset is mainly on the valence band, the electrons in the conduction band is less scattered by the conduction band discontinuity, as compared to holes in the valence band with large valence band discontinuity. The dark current of Si, Ge, Ge quantum dot, and $Si_{0.8}Ge_{0.2}$ multi-layer MOS devices are shown in Fig. 9. Note that the complex structure of valence band due to the wetting layer and quantum dots has little effects on our NMOS, where electron transport dominates. The dark current is mainly determined by thermal generation through the defects in the deep depletion region and the interface states. Thus, the Ge quantum dot device with a smaller bandgap has a larger dark current, as compared to the Si device.

Fig. 10, Fig. 11, and Fig. 12 are the responsivity and efficiency of devices under 820, 1300 and 1550 nm lightwave exposure, respectively. For 820 nm detection, the Ge quantum dot device has a very high external quantum efficiency (20%) similar to the Ge device. With the insertion of Ge quantum dots, the efficiency increases by a factor 10 as compared to the Si device. All the efficiency reported here is the external quantum efficiency. Due to the reflection of Si (~35 % at 820 nm) and the coupling loss, the internal quantum efficiency should reach 30%. This indicates extremely low defect density is formed during the UHV/CVD growth as well as the LPD process, and the defect-related recombination (if any) does not seriously degrade the efficiency. The dark current is as low as 0.06 mA/cm^2 for Ge quantum dot devices, while the dark current of typical Ge pin devices is 20 mA/cm^2 (7). For 1300 nm detection wavelength (Fig. 11), the responsivity of Ge quantum dot devices drops to 0.16 mA/W, due to the insufficient thickness of active layers, while Ge devices still have the responsivity of 100 mA/W. The responsivity of $Si_{0.8}Ge_{0.2}$ multi-layers is only 0.04 mA/W, due to the small Ge fraction in the films. For 1550nm detection (Fig. 12), the responsivity of the Ge quantum dot devices is 0.08 mA/W, while the responsivity of Ge devices is still around 75 mA/W. The quantum dot MOS detectors can also be operated at 850 nm (not shown here) with high responsivity (> 300 mA/W). Note that the LPD oxide quality affects the device performance a lot. Therefore, to have best device performance, both the LPD process and the quantum dot structures should be optimized.

Conclusions

The MOS Ge quantum dot device can detect the wavelength of 820 nm, 1300 nm, and 1550 nm, with the responsivity of 130, 0.16, and 0.08 mA/W, respectively. The bias voltage can be as low as zero volt. The dark current is as low as 0.06 mA/cm^2. The detection efficiency of quantum dot device at 820 nm is close to the Ge device. The high performance of Ge quantum dot MOS detectors with LPD oxide at 820 nm makes it feasible to integrate optoelectronic devices into the Si chip for short-reach optical communication.

Acknowledgments

The authors would like to acknowledge Chun Liang Lin and Prof. Lon A. Wang of Optical Fiber Communication and Sensor Lab (OFC&S), Department of Electrical Engineering, National Taiwan University for the responsivity measurement of the Ge MOS detector. This work is partially supported by National Science Council, ROC, under contract nos. (91-2120-E-002-007, and 91-2215-E-002-027)

References

(1) R. A. Soref, "Silicon-based Optoelectronics," *Proc. IEEE*, vol. 81, no. 12, pp. 1687-1706, 1993.
(2) Min Yang et al., "High Speed Silicon Lateral Trench Detector on SOI Substrate," *IEDM Tech. Dig.*, pp.547-550, 2001.
(3) C. W. Liu, W. T. Liu, M. H. Lee, W. S. Kuo, and B. C. Hsu, "A Novel Photodetector Using MOS Tunneling Structures," *IEEE Electron Device Lett.*, vol. 21, no. 6, pp. 307-309, 2000.
(4) T. I. Kamins, D. A. A. Ohlberg, R. S. Williams, W. Zhang, and S. Y. Chou, "Positioning of self-assembled, single-crystal, germanium islands by silicon nanoimprinting," *Appl. Phys. Lett.*, vol. 74, pp. 1773-1775, 1999.
(5) H. Nagayama, H. Honda, and H. Kawahara, "A New Process for Silica Coating," *J. Electrochem. Soc.*, vol. 135, p. 2013, 1988.
(6) Jenq-Shiuh Chou and Si-Chen Lee, "Improved process for liquid phase deposition of silicon dioxide,"*Appl. Phys. Lett.*, vol. 64 , pp. 1971-1973, 1994.
(7) S. Fama, L. Colace, G. Masini, G. Assanto, and Hsin-Chiao Luan, "High performance germanium-on-silicon detectors for optical communications," *Appl. Phys. Lett.*, vol. 81, no. 4, pp. 586-588, 2002.

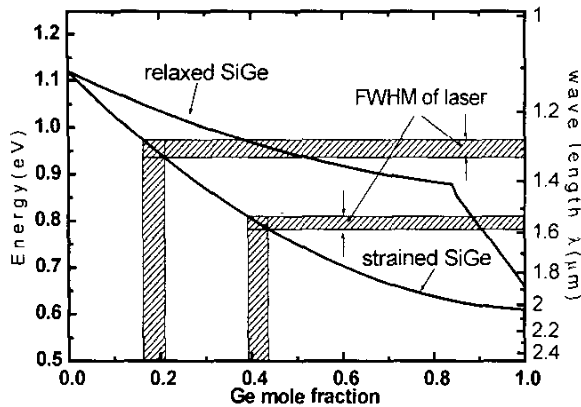

Fig.1 The bandgap and cut-off wavelength vs Ge mole fraction. As Ge mole fraction increases, the maximum absorption wavelength also increases. The shadowed area represents the laser bandwidth in our experiment.

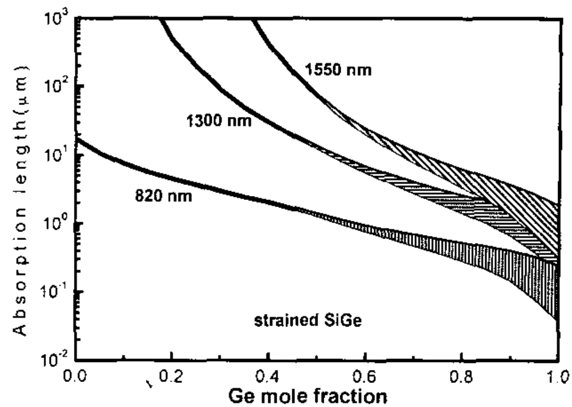

Fig.2 The absorption length at 820, 1300, and 1550 nm vs Ge mole fraction. The absorption length decreases as the Ge mole fraction increases. For the large Ge fraction, the shadowed areas indicate the uncertainty of the estimation.

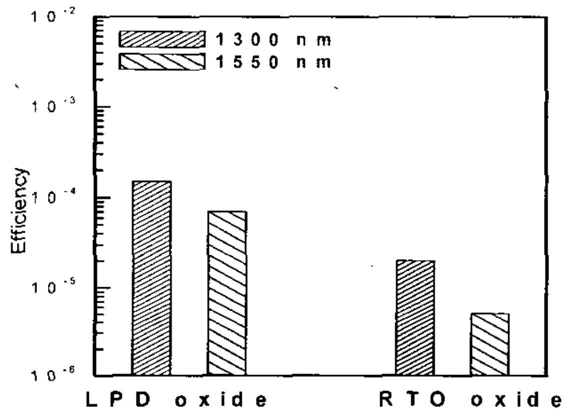

Fig. 3 The characteristics of Ge quantum dot detectors with RTO and LPD oxide. The MOS detector with RTO oxide has low efficiency.

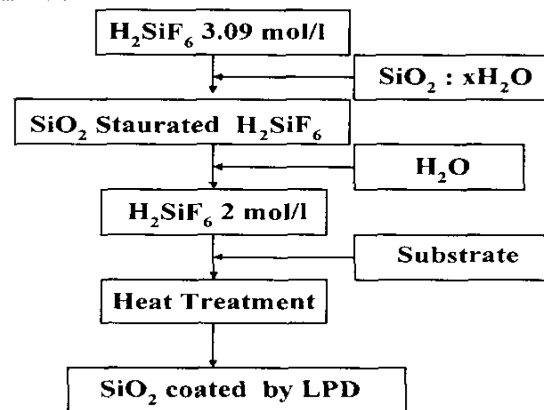

Fig. 4 The process flow of the liquid phase deposition.

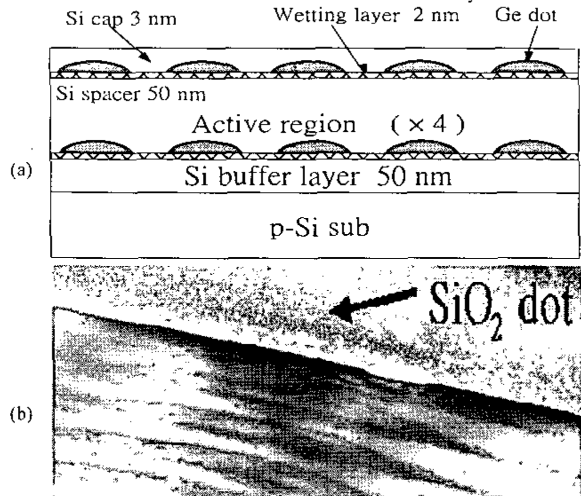

Fig. 5 (a) The structure of 5-layer Ge quantum dot devices prepared by UHV/CVD. Note that the top Ge quantum dots have a Si cap of 3 nm. (b) The TEM photograph.

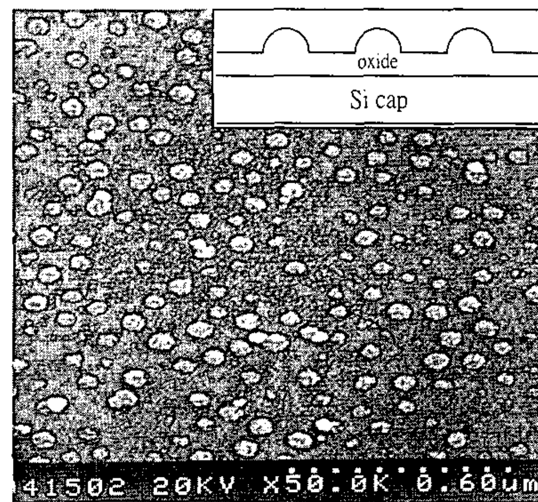

Fig. 6 The SEM morphology of quantum dot samples after the LPD process. The strain induced oxide dots are deposited directly on self-assembled Ge islands.

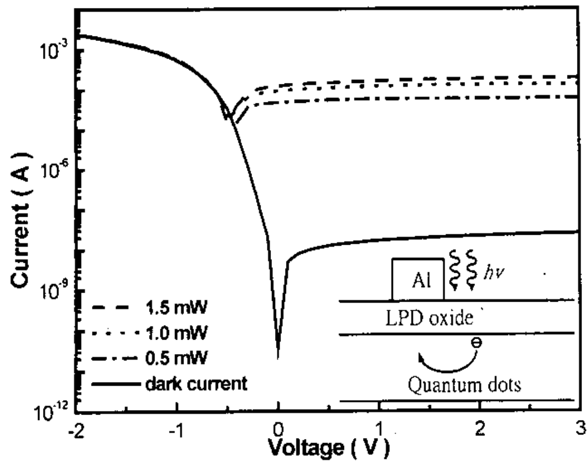

Fig. 7 The I-V characteristics of a quantum dot MOS detector under 820 nm lightwave exposure. The photo-generated carriers can be collected by gate electrode through the lateral drift and diffusion.

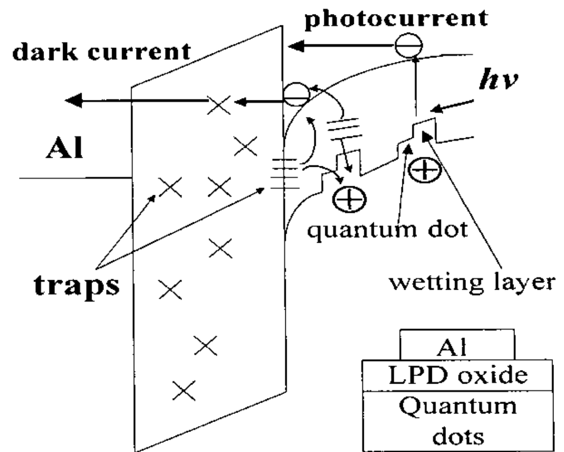

Fig. 8 The band diagram of a Ge quantum dot NMOS detector under inversion bias and the device structure. The photo-generated electrons tunnel through LPD oxide.

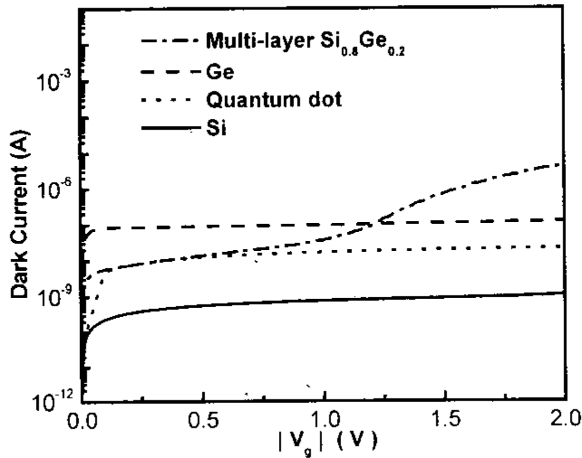

Fig. 9 The dark current of all 4 devices with LPD oxide.

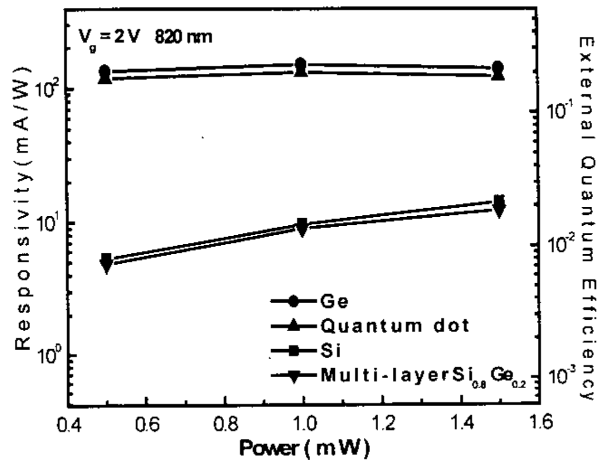

Fig. 10 The responsivity and efficiency at 820 nm. The Ge quantum dot device has a similar efficiency to Ge device.

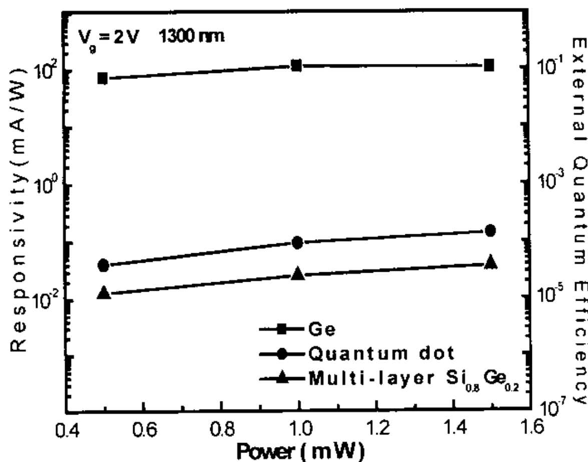

Fig.11 The responsivity and efficiency at 1300 nm. The efficiency of quantum dot detectors is larger than multi-layer $Si_{0.8}Ge_{0.2}$ detectors.

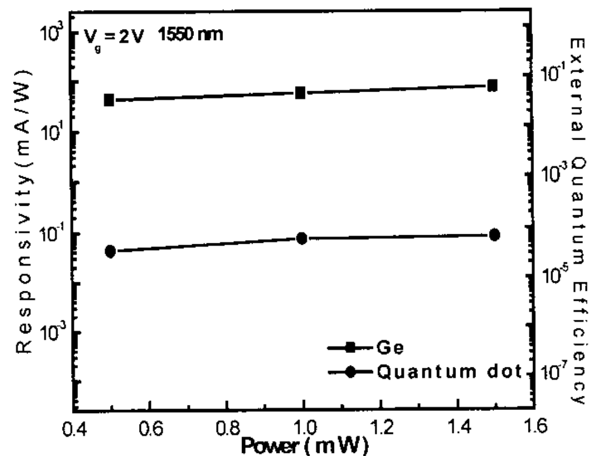

Fig.12 The responsivity and efficiency at 1550 nm. Only Ge and Ge quantum dot detectors have response at 1550 nm.